Elnaz Jamili, Amit C. Nathwani and Vivek Dua*

14 Model-based dose selection for gene therapy for haemophilia B

Abstract: Haemophilia B, also known as the Christmas disease, named after Stephen Christmas the first patient diagnosed with this disease, is an inherited disease caused by a defect in the Factor IX Gene (*F9*). This defect manifests in insufficient production of the blood coagulation factor IX, resulting in excessive bleeding. The therapy which is mainly used involves prophylactic infusions of factor IX concentrate to improve the quality of life by minimising the episodes of bleeds. The main limitations of such a treatment plan are repeat infusions, product half-life, costs and inhibitor formation. The FIX concentration in healthy individuals is typically 90 nM and based upon the experience of the clinicians increasing FIX activity to 1–5 % of normal values has significant impact on patients' quality of life. Therefore, even a partial correction the FIX deficiency would result in improved clinical outcomes and increase the chances of patients living a near-normal life. Gene therapy has the potential to deliver this, and the fact that haemophilia B is monogenic in nature further encourages the exploration of gene delivery for this disease. In this chapter, an integrated Pharmacokinetic (PK) – Pharmacodynamic (PD) model that has been developed using the clinical data is reported. The key features of the model are that it considers the pharmacological response, i.e., plasma FIX coagulation activity level as well as the toxicological response, i.e., the level of serum alanine aminotransferase. The simulation-based PK-PD modelling approach is then used for the initial dose selection to provide clinicians with better tools to simplify the decision-making process for designing more effective treatment plans, which can be tailored to maximise efficacy while minimising toxicity for individual patients.

Keywords: gene delivery; initial dose selection; Pharmacokinetic/pharmacodynamic modelling; toxicity; efficacy

***Corresponding author: Vivek Dua**, Department of Chemical Engineering, The Sargent Centre for Process Systems Engineering, University College London, Torrington Place, London WC1E 7JE, UK,
E-mail: v.dua@ucl.ac.uk. https://orcid.org/0000-0002-0165-7421

Elnaz Jamili, Department of Chemical Engineering, Centre for Process Systems Engineering, University College London, Torrington Place, London, WC1E 7JE, UK

Amit C. Nathwani, Department of Haematology, UCL Cancer Institute, University College London, London, UK

As per De Gruyter's policy this article has previously been published in the journal Physical Sciences Reviews. Please cite as: E. Jamili, A. C. Nathwani and V. Dua "Model-based dose selection for gene therapy for haemophilia B" *Physical Sciences Reviews* [Online] 2024. DOI: 10.1515/psr-2024-0057 | https://doi.org/10.1515/9783111394558-014

14.1 Introduction

14.1.1 Chemical engineering and haemophilia B

This chapter presents the collaborative work that was carried out by researchers from chemical engineering and haemophilia at University College London [1]. The problem statement and steps for developing gene therapy for haemophilia B involve statements that chemical engineers are quite familiar with. It is common for chemical engineers to collect experimental data for the process system under consideration, set up a mathematical model that captures the phenomena taking in the process system and then estimate parameters for the mathematical model that fit the data that were collected. If the data does not fit well, usually the mathematical model is revisited and/or additional experiments are carried out, in an iterative manner, until there is sufficient confidence in the model. The model is then simulated to predict system response for situations that were not necessarily covered during experimentation. This aligns with the decision that a clinician would have to take in terms of selecting dose for gene delivery for haemophilia B. While higher dose would result in higher efficacy, it would also give higher toxicity, making it a multi-objective decision-making problem. Decision making in chemical engineering also involves similar situations where, for example, one has to consider trade-offs between profit and environmental impact, yield and safety, etc. In this chapter, clinical data can be considered to be equivalent to the experimental data and integrated pharmacokinetic/pharmacodynamic model can be considered to be equivalent to the mathematical model, mentioned above.

14.1.2 Haemophilia B

Haemophilia B (HB) is a genetic bleeding disorder resulting from a deficiency or dysfunction of coagulation factor IX (FIX) caused by mutations in the gene that encodes FIX [2, 3]. Although prophylactic therapy with factor IX protein concentrates improves clinical outcomes and reduces the frequency of spontaneous bleeding, it requires frequent intravenous injections for the life-time of patients due to the short half-life of the protein, resulting in an inconvenient and expensive (£140,000 per year per patient) treatment [4]. Thus, various strategies have been investigated for the treatment of haemophilia B including the use of bioengineered coagulation factors [5] and gene-transfer therapy [6, 7]. Gene therapy is a potentially curative treatment option as it aims to restore, modify or enhance cellular functions through the introduction of a therapeutic gene into a target cell, which is demonstrated in the work by Nathwani et al. [7–13]. In the clinical trial conducted by Nathwani and colleagues, a single dose of a serotype-8-pseudotyped, self-complementary (sc) adeno-associated (AAV) vector expressing a codon-optimised version of the human factor IX (hFIXco) gene was infused in patients with severe HB whose FIX activity level is <1 % of normal values [12, 13]. hFIXco transgene was

synthesised and cloned downstream of a compact synthetic liver-specific promoter (LP1) to enable packaging into scAAV vectors (scAAV2/8-LP1-hFIXco) [4]. The evaluation of safety and efficacy in HB patients, having had the peripheral-vein infusion of scAAV2/8-LP1-hFIXco, was reported in the work by Nathwani et al. [7].

Mathematical models are crucial tools for understanding the key mechanisms involved in biological systems, and for predicting the outcome of a given treatment plan. Mathematical modelling for gene delivery systems has evolved over the years, starting with the work by Ledley and Ledley [14] in which the authors developed a multi-compartment mathematical model for studying the kinetics of cellular processes. A variety of studies have illustrated how mathematical models can be applied to gene delivery systems. Most of the works have focused on the concept of mass action kinetic model to study the critical steps involved in the process [14–17]. A number of different computational methodologies have provided insights into the gene delivery process, including stochastic simulations [18], quantitative structure–activity relationship (QSAR) modelling strategy [19], mechanistic spatio-temporal and stochastic model of DNA delivery [20], semi-mechanistic model of transgene expression [21] and telecommunication model [22].

While a lot of important work has been done in the area of modelling for gene delivery systems, there are several areas that are yet to be explored adequately. We have recently developed a model-based control algorithm for both efficacy and safety to provide quantitative understanding of non-viral siRNA delivery [23]. Having explored the nature and purpose of quantitative analysis of *in vitro* experimental data in our previous work, this chapter aims to develop a novel mathematical modelling approach, based on *in vivo* clinical data, for gene transfer of adeno-associated viral vectors in patients with haemophilia B. In this work, an integrated pharmacokinetic/pharmacodynamic model is developed using compartment modelling to describe the behaviour of scAAV2/8-LP1-hFIXco vectors in patients, which is then used in a simulation-based modelling platform for the initial dose selection with the goal of predicting the pharmacokinetics and pharmacodynamics of the vector during the therapy. A promising platform for gene delivery systems is provided by using modelling techniques to determine the initial dose selection that can be used in clinical trial simulations to determine optimal dosing recommendations.

14.2 Methods

14.2.1 Clinical data

Nathwani et al. [7] aimed to assess the efficacy and safety of factor IX gene therapy in patients with severe HB by evaluating the stability of transgene expression and monitoring the hepatocellular toxicity. The authors also reported the vector genomes in plasma, urine, stool, semen and saliva, which were collected from patients at regular intervals in order to assess vector shedding following systemic administration of scAAV2/

8-LP1-hFIXco. The clinical data are used to build an integrated PK/PD model so as to be capable of providing a platform to guide initial dose selection.

14.2.2 Pharmacokinetic modelling

Physiologically based pharmacokinetic (PBPK) models, while being able to offer a more realistic picture of vector kinetics by modelling the real physiological space in the human body, are very complex and typically require more clinical data in more compartments for the validation of the models, which is not readily available in clinical trials [24]. Therefore, a mechanistically lumped PK model was developed based on the available clinical data. The PK model comprised of two compartments, plasma (P) and body fluids (BFs), to illustrate the simultaneous kinetics of both plasma and metabolites (Figures 14.1 and 14.2). The body fluids, which encompass data from urinary, stool, semen and saliva, were lumped into a single compartment to represent the elimination process. This approach was adopted because the parallel effluxes can be merged and represented within a unified compartment [24, 25]. Mathematically,

$$\frac{dC_P}{dt} = -\theta_d\, C_P - \theta_{el.0}\, C_P \tag{14.1}$$

$$C_P\,(t=0) = C_{P0}$$

$$\frac{dC_{BF}}{dt} = \theta_{el.0}\, C_P - \theta_{el.1}\, C_{BF} \tag{14.2}$$

$$C_{BF}\,(t=0) = C_{BF0}$$

where C_P (vector genome/mL) and C_{BF} (vector genome/mL) are the vector concentrations in patient plasma and body fluids, respectively. θ_d (day^{-1}) represents the distribution rate constant while $\theta_{el.0}$ (day^{-1}) and $\theta_{el.1}$ (day^{-1}) are the elimination rate constants.

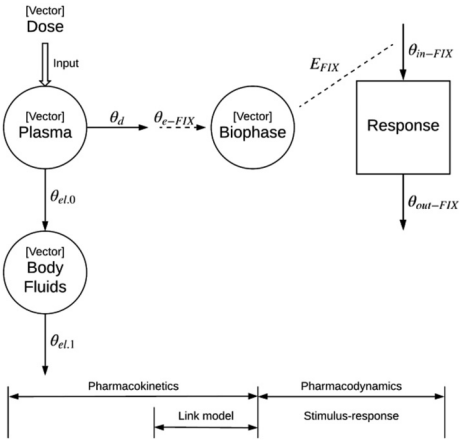

Figure 14.1: Schematic representation illustrating the relationship between kinetics and dynamics of the vector when considering the pharmacological response (plasma FIX coagulation activity level).

The developed pharmacokinetic model serves as a platform for a quantitative evaluation of gene delivery. Equation (14.1) captures the rate of change of the vector concentration in patient plasma after a single intravenous infusion of vector.

14.2.3 Pharmacodynamic modelling

Human factor IX (hFIX) is a coagulation protein, which is synthesised in the liver and encoded in a gene located on the X chromosome [26, 27]. Hepatocytes, which are the most common cells type in the liver, directly secrete factor IX into the bloodstream, where it circulates in an inactive form until needed in a response to an injury that damages the blood vessel wall [28]. Since FIX is naturally synthesised in the liver, the site of action for scAAV2/8-LP1-hFIXco vectors is located in the liver compartment.

In order to develop a mathematical model, the plasma FIX activity has been considered as the pharmacological effect (response), which can be treated as an objective function to be maximised in a gene delivery optimal control problem. A physiological indirect response model with stimulation of factors controlling the response was thought to be appropriate to describe the vector pharmacodynamics. This is because of the time delay between the observed pharmacological effects and vector concentration in plasma as the pharmacological responses take time to be developed. The temporal displacement could be due to the vector tissue distribution phenomena to reach the site of action, liver. To this purpose, a dynamic model must be developed to link the vector concentration in the biophase or effect compartment to a response compartment. The effect compartment model, which is also known as the link model, can be considered as a first-order distribution model relating the vector concentration in plasma and the biophase using a first-order constant. Once the vector is transferred to the liver, a cascade of biological events may take place resulting in a functional response, which can be viewed as a link model. Schematic illustration of the integrated PK/PD model is shown in Figure 14.1.

While a more detailed representation of an integrated PK/PD approach can be developed by incorporating the liver compartment into the PK model, the model structure, which was developed and used in this work, had been simplified to only include the plasma and other body fluids compartments. This is due to a lack of available data as liver biopsies are required.

Considering the pharmacological analysis, the rate of change of the vector concentration in the effect (biophase) compartment, C_{e_FIX} (vector genome/mL), can be modelled as:

$$\frac{dC_{e\_FIX}}{dt} = \theta_{e\_FIX}\, C_P - \theta_{in\_FIX}\, C_{e\_FIX} \tag{14.3}$$

where C_P (vector genome/ml) is the concentration of vector in the plasma compartment of the pharmacokinetic model, linked to the effect compartment, with the first-order rate constant $\theta_{e\_FIX}\left(\text{day}^{-1}\right)$.

The plasma FIX coagulation activity level, R_{FIX} (% of the normal value – IU/deciliter), which is of interest in our case, is formulated as a function of the concentration in the effect compartment with the use of an effect-concentration model. The differential equation for the observed pharmacological effect, factor IX activity level, can be expressed as:

$$\frac{dR_{FIX}}{dt} = \theta_{in\_FIX}\, E_{FIX} - \theta_{out\_FIX}\, R_{FIX} \tag{14.4}$$

where the *rate in* and *rate out* of the response compartment are governed by $\theta_{in\_FIX}\left(\text{day}^{-1}\right)$ and $\theta_{out\_FIX}\left(\text{day}^{-1}\right)$.

Note that the effect compartment model should be selected with an appropriate effect equation. In this study, the response is modelled by means of a linear transduction function in which the vector concentration is proportionally related to a pharmacological response [29]. Therefore,

$$E_{FIX} = k\, C_{e\_FIX} \tag{14.5}$$

where k is the slope parameter, which is assumed to be $k = 1$ in order to simplify the model to help to mitigate the numerical difficulties.

14.2.4 Incorporating the toxicological model

The PD model may be extended to incorporate the toxicological responses that capture the liver toxicity, which was observed in the clinical study by Nathwani and colleagues as the primary endpoint of their study was the safety evaluation of the vector infusion at different doses. The reported level of serum alanine aminotransferase (ALT) over time demonstrates the hepatocellular toxicity. ALT is an enzyme which is found in serum and organ tissues such as liver. The ALT level is the most widely used clinical biomarker of liver function, which may be elevated as a result of the leakage from the damaged hepatocytes into the plasma following hepatocellular injury [30].

In this section, the structure of the PD model has been kept the same as in Section 14.2.3. Assuming an indirect response model with stimulation of factors controlling the toxicological response (Figure 14.2), the rate of change of the vector concentration in the effect (biophase) compartment, C_{e_ALT} (vector genome/mL), can be modelled as:

$$\frac{dC_{e\_ALT}}{dt} = \theta_{e\_ALT}\, C_P - \theta_{in\_ALT}\, C_{e\_ALT} \tag{14.6}$$

where C_P (vector genome/mL) is the concentration of vector in the plasma compartment of the pharmacokinetic model, linked to the effect compartment, with the first-order rate constant $\theta_{e\_ALT}\left(\text{day}^{-1}\right)$.

The ALT level, R_{ALT} (IU/L), is formulated as a function of the concentration in the effect compartment with the use of an effect-concentration model:

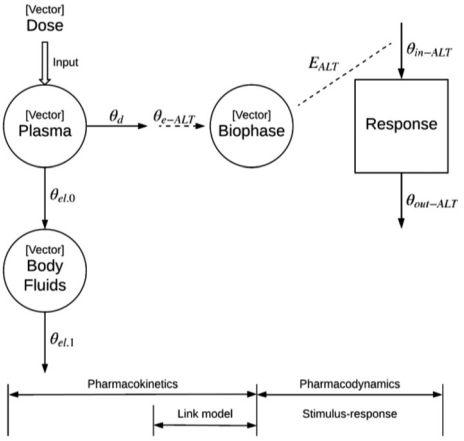

Figure 14.2: Schematic representation illustrating the relationship between kinetics and dynamics of the vector when considering the toxicological response (ALT level).

$$\frac{dR_{ALT}}{dt} = \theta_{in\_ALT}\, E_{ALT} - \theta_{out\_ALT}\, R_{ALT} \tag{14.7}$$

$$E_{ALT} = k\, C_{e\_ALT} \tag{14.8}$$

where the *rate in* and *rate out* of the response compartment are governed by $\theta_{in\_ALT}\left(\text{day}^{-1}\right)$ and $\theta_{out\_ALT}\left(\text{day}^{-1}\right)$, and $k = 1$.

14.3 Results and discussion

The proposed modelling framework will be evaluated for three patients with severe HB who had received intermediate dose of vector, 6×10^{11} vector genomes (vg) per kilogram (kg) of body weight, (patient 4), and high dose of vector, 2×10^{12} vg per kg, (patients 6 and 9). The mean weight was 80.7 kg. Table 14.1 summarises the key characteristics of the patients.

Table 14.1: Key characteristics of the patients at baseline, according to vector dose. Adapted from Nathwani et al. [7].

Characteristic	Vector dose, 6×10^{11} vg/kg	Vector dose, 2×10^{12} vg/kg	
	Patient 4	Patient 6	Patient 9
Sex	Male	Male	Male
Age (yr)	29	27	44
Factor IX prophylaxis	Once weekly	Three times weekly	On demand
HIV status	Negative	Negative	Negative
Hepatitis C status	Negative	Negative	Positive

The results obtained from this study will be presented in two parts. First, the results of the parameter estimation problem will be discussed in Section 14.3.1. Then, a number of dynamic simulations will be presented in Section 14.3.2 for initial dose selection.

14.3.1 Parameter estimation

Having the clinical data and the PK/PD model, given by Equations (14.1)–(14.8), the parameter estimation problem was formulated as an optimisation problem and solved using the analytical solutions of the PK and PD models, which were obtained by using Mathematica. Since the spread of values in the PK clinical data set is large, the PK parameter estimation problem was performed using both absolute and scaled objective functions. The full set of model parameters and state variables are listed in Table 14.2.

The generic mathematical formulation of the parameter estimation problem is as follows:

Table 14.2: Model parameters and state variables of the PK/PD model.

Symbol	Description	Units
Ψ_k	The vector of the state variables in compartment k	
C_P	Vector concentration in the plasma compartment	vg/mL
C_{BF}	Vector concentration in the body fluids compartment	vg/mL
C_{e_FIX}	Vector concentration in the biophase (effect) compartment when considering the pharmacological response (FIX coagulation activity level)	vg/mL
C_{e_ALT}	Vector concentration in the biophase (effect) compartment when considering the toxicological response (ALT level)	vg/mL
R_{FIX}	Plasma factor IX coagulation activity level	IU/dL
R_{ALT}	ALT level	IU/L
θ	The vector of the model parameters	
θ_d	Distribution rate constant	day^{-1}
$\theta_{el.0}$	Elimination rate constant	day^{-1}
$\theta_{el.1}$	Elimination rate constant	day^{-1}
θ_{e_FIX}	Rate constant linking a kinetic model and a dynamic model when considering the pharmacological response (FIX coagulation activity level)	day^{-1}
θ_{e_ALT}	Rate constant linking a kinetic model and a dynamic model when considering the toxicological response (ALT level)	day^{-1}
θ_{in_FIX}	The *rate in* of the pharmacological response compartment (R_{FIX})	day^{-1}
θ_{out_FIX}	The *rate out* of the pharmacological response compartment (R_{FIX})	day^{-1}
θ_{in_ALT}	The *rate in* of the toxicological response compartment (R_{ALT})	day^{-1}
θ_{out_ALT}	The *rate out* of the toxicological response compartment (R_{ALT})	day^{-1}
$Err_{absolute}$	Absolute objective function	
Err_{scaled}	Scaled objective function	
$\widehat{\Psi}_k$	The vector of the observed clinical data in compartment k	

$$\mathrm{Err}_{\mathrm{absolute}} = \min_{\boldsymbol{\theta},\boldsymbol{\Psi}(t)} \sum_{p\in P} \sum_{k\in K} \left\{ \boldsymbol{\Psi}_k(t_p) - \widehat{\boldsymbol{\Psi}}_k(t_p) \right\}^2 \tag{14.9}$$

or

$$\mathrm{Err}_{\mathrm{scaled}} = \min_{\boldsymbol{\theta},\boldsymbol{\Psi}(t)} \sum_{p\in P} \sum_{k\in K} \left\{ \frac{\boldsymbol{\Psi}_k(t_p) - \widehat{\boldsymbol{\Psi}}_k(t_p)}{\widehat{\boldsymbol{\Psi}}_k(t_p)} \right\}^2 \tag{14.10}$$

subject to the analytical solutions of the PK/PD model. For more details, please see Equations (14.1)–(14.6) in the Supplementary Appendix.

To carry out parameter estimation for the system, first, PK/PD parameters were estimated individually for each patient, which could be useful for the development of personalised gene therapy. Then, PK and PD parameters were estimated for all patients simultaneously, which were used for the initial dose selection, aiming at predicting the physiological response of a patient to a dose of vector. For individually estimated PK/PD parameters, the analysis was dependent on the initial vector concentration, whereas the simultaneous parameter estimation was dose-dependent. Tables 14.3 and 14.4 summarise the parameter estimation results for individually and simultaneously estimated parameters. The estimated parameter values were then used for dynamic simulations using Orthogonal Collocation on Finite Elements (OCFE), which were carried out for the validation of the model, with a view to pave the way for control of gene delivery in future work. Note that the model parameters are specific to a patient and may vary between patients (inter-patient) and also within individual patients (intra-patient). There are different factors that affect inter- and intra-patient variability, such as age, sex, body weight, health condition and activity levels.

In order to visualise the variance between the estimated PK/PD parameters across different patients, the results are also graphically shown in Figure 14.3. Note that in the following figure, P.4, P.6 and P.9 refer to Patient 4, Patient 6 and Patient 9, respectively, where the PK and PD parameters were estimated individually for each patient. However, P.4-6-9 refers to the population modelling approach in which each PK and PD parameters were estimated for all patients simultaneously.

In Figure 14.3, the variability of the estimated model parameters across different patients could be associated with the inter-patient variability, suggesting that the personalised gene therapy using an individual modelling approach would make more sense because the pharmacokinetics and pharmacodynamics of the vector can vary between patients. However, to gain more insights into the process, both the individual modelling approach (solving the parameter estimation problem for each patient individually) and the population modelling approach (solving the parameter estimation problem for all patients simultaneously) were considered in the present work.

It is important to note here that the estimated model parameters could vary for different initial guesses used for the parameter estimation problem. Difficulties arise from both the existence of local minima and non-identifiability [31]. The solver may find different local minima when started from different starting points due to the non-

Table 14.3: Estimated PK/PD model parameters, individually for each patient.

		Patient 4 (P.4)		
		Estimated parameters (day^{-1})		
PK model	Absolute OBJ[a]	θ_d = 1.5710559	$\theta_{el.0}$ = 1.0506840	$\theta_{el.1}$ = 2.1366106
	Scaled OBJ[b]	θ_d = 2.5971076	$\theta_{el.0}$ = 0.0247028	$\theta_{el.1}$ = 0.4823376
PD model	FIX	$\theta_{e\_FIX} = 9.7701316$	$\theta_{in\_FIX} = 0.0016288$	$\theta_{out\_FIX} = 0.0631596$
	ALT	$\theta_{e\_ALT} = 18.4752261$	$\theta_{in\_ALT} = 0.0005428$	$\theta_{out\_ALT} = 0.0074621$
		Patient 6 (P.6)		
		Estimated parameters (day^{-1})		
PK model	Absolute OBJ[a]	θ_d = 2.1140705	$\theta_{el.0}$ = 0.0073093	$\theta_{el.1}$ = 0.5635716
	Scaled OBJ[b]	θ_d = 2.0194024	$\theta_{el.0}$ = 0.0910754	$\theta_{el.1}$ = 1.7344535
PD model	FIX	$\theta_{e\_FIX} = 21.1668725$	$\theta_{in\_FIX} = 0.0003748$	$\theta_{out\_FIX} = 0.0158966$
	ALT	$\theta_{e\_ALT} = 0.3656878$	$\theta_{in\_ALT} = 0.0028681$	$\theta_{out\_ALT} = 0.0005408$
		Patient 9 (P.9)		
		Estimated parameters (day^{-1})		
PK model	Absolute OBJ[a]	θ_d = 0.1593991	$\theta_{el.0}$ = 1.1246204	$\theta_{el.1}$ = 0.6580731
	Scaled OBJ[b]	θ_d = 0.9911402	$\theta_{el.0}$ = 0.3439847	$\theta_{el.1}$ = 0.4674078
PD model	FIX	$\theta_{e\_FIX} = 2.0086934$	$\theta_{in\_FIX} = 0.0012088$	$\theta_{out\_FIX} = 0.0038267$
	ALT	$\theta_{e\_ALT} = 6.4510203$	$\theta_{in\_ALT} = 0.0010856$	$\theta_{out\_ALT} = 0.0033077$

[a]Solved the parameter estimation problem using an absolute objective function (Equation (14.9)). [b]Solved the parameter estimation problem using a scaled objective function (Equation (14.10)).

Table 14.4: Estimated PK/PD model parameters, for all patients simultaneously.

		Patients 4, 6 and 9 (P.4-6-9)		
		Estimated parameters (day^{-1})		
PK model	Absolute OBJ[a]	θ_d = 1.5511141	$\theta_{el.0}$ = 0.4723049	$\theta_{el.1}$ = 0.7640243
	Scaled OBJ[b]	θ_d = 7.1957447	$\theta_{el.0}$ = 2.0910047	$\theta_{el.1}$ = 1.7113180
PD model	FIX	$\theta_{e\_FIX} = 11.2140501$	$\theta_{in\_FIX} = 0.0005731$	$\theta_{out\_FIX} = 0.0737731$
	ALT	$\theta_{e\_ALT} = 0.6582939$	$\theta_{in\_ALT} = 0.0007284$	$\theta_{out\_ALT} = 0.0014742$

[a]Solved the parameter estimation problem using an absolute objective function (Equation (14.9)). [b]Solved the parameter estimation problem using a scaled objective function (Equation (14.10)).

convexity of the objective function. Global optimisation-based algorithms were applied; however, the model was unable to converge to find a global optimal solution. Furthermore, the identifiability issue is concerned with the theoretical existence of unique solutions to the parameter estimation problem. Hence, there are various sets of parameter values that fit the clinical data equally well. Different strategies, such as model

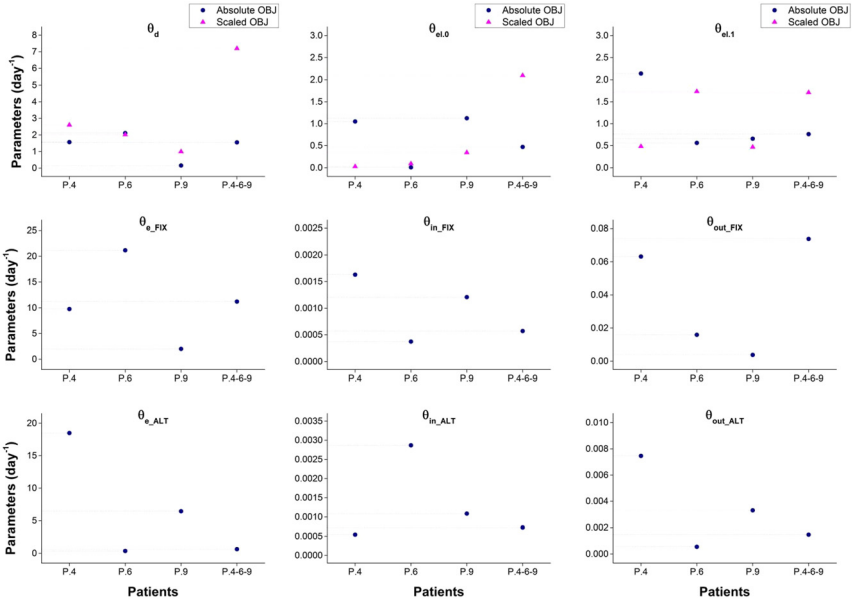

Figure 14.3: Estimated PK/PD parameters across different patients.

reformulation, model reduction, or generating additional clinical data can be used to overcome the identifiability problem [31]. Sensitivity analysis was performed to investigate the sensitivities of state variables relative to small changes in model parameters at the steady state (Tables 14.5 and 14.6). All relative sensitivities of model variables to changes in parameters are smaller than one in absolute value, meaning that perturbations in value of the parameters are attenuated.

The results obtained from the PK/PD analysis using an individual modelling are shown in Figures 14.4–14.6, while the results illustrated in Figures 14.7–14.9 present the PK/PD analysis using a population modelling. The parameter estimation and the simulation results obtained from the work have been qualitatively verified by using the compartmental modelling approach. As can be seen from the following figures, the dynamic simulations agree closely with the parameter estimation results, and the model predictions are in good accordance with the clinical data. However, depending on the type of the objective function and the choice of individual modelling approach or population modelling approach, various results of the study highlighted several feasible configurations of the system. Such considerations were taken into account to aid decision making for further research. The values of the objective function obtained for each case study are reported in Tables 14.7 and 14.8, which give an indication of the solution accuracy. According to the results, the objective function values observed for the PD parameter estimation are much higher than those obtained for the PK parameter estimation. This is because of the extensive PD data set and the widespread existence of

Table 14.5: Model sensitivity matrix for the individual modelling approach.

Parameters	Individual modelling approach											
	Patient 4				Patient 6				Patient 9			
	C_P	C_{BF}	R_{FIX}	R_{ALT}	C_P	C_{BF}	R_{FIX}	R_{ALT}	C_P	C_{BF}	R_{FIX}	R_{ALT}
$\theta_{d\_absolute}$	−0.000001	−0.000001	–	–	−0.000002	−0.000001	−0.2	−0.14	−0.000001	−0.000001	−0.03	−0.08
$\theta_{el.0\_absolute}$	−0.000001	−0.000001	–	–	−0.000001	0.000001	−0.01	−0.01	−0.000002	−0.000001	−0.18	−0.57
$\theta_{el.1\_absolute}$	–	−0.000002	–	–	–	−0.000003	–	–	–	−0.000002	–	–
θ_{d_scaled}	−0.000002	−0.000003	−0.04	−0.6	−0.000002	−0.000001	–	–	−0.000002	−0.000001	–	–
$\theta_{el.0\_scaled}$	−0.000001	0.000002	−0.01	−0.01	−0.000001	0.000001	–	–	−0.000001	0.000001	–	–
$\theta_{el.1\_scaled}$	–	−0.000025	–	–	–	−0.000002	–	–	–	−0.000002	–	–
θ_{e_FIX}	–	–	0.03	–	–	–	0.18	–	–	–	0.18	–
θ_{in_FIX}	–	–	−0.03	–	–	–	0.11	–	–	–	0.17	–
θ_{out_FIX}	–	–	−0.04	–	–	–	−0.21	–	–	–	−0.27	–
θ_{e_ALT}	–	–	–	0.57	–	–	–	0.12	–	–	–	0.62
θ_{in_ALT}	–	–	–	0.3	–	–	–	−0.02	–	–	–	0.48
θ_{out_ALT}	–	–	–	−0.68	–	–	–	−0.44	–	–	–	−0.81

Table 14.6: Model sensitivity matrix for the population modelling approach.

Parameters	Population modelling approach											
	Patient 4				Patient 6				Patient 9			
	C_P	C_{BF}	R_{FIX}	R_{ALT}	C_P	C_{BF}	R_{FIX}	R_{ALT}	C_P	C_{BF}	R_{FIX}	R_{ALT}
$\theta_{d\_absolute}$	−0.000002	−0.000001	−0.03	−0.1	−0.000002	−0.000001	−0.15	−0.53	−0.000002	−0.000001	−0.22	−0.49
$\theta_{el.0\_absolute}$	−0.000001	0.000001	−0.01	−0.03	−0.000001	0.000001	−0.05	−0.16	−0.000001	0.000001	−0.07	−0.15
$\theta_{el.1\_absolute}$	–	−0.000002	–	–	–	−0.000004	–	–	–	−0.000002	–	–
θ_{d_scaled}	−0.000001	−0.000001	–	–	−0.000001	−0.000001	–	–	−0.000001	−0.000001	–	–
$\theta_{el.0\_scaled}$	−0.000001	0.000001	–	–	−0.000001	0.000001	–	–	−0.000001	0.000001	–	–
$\theta_{el.1\_scaled}$	–	−0.000002	–	–	–	−0.000002	–	–	–	−0.000002	–	–
θ_{e_FIX}	–	–	0.03	–	–	–	0.17	–	–	–	0.27	–
θ_{in_FIX}	–	–	0.01	–	–	–	0.05	–	–	–	0.19	–
θ_{out_FIX}	–	–	−0.04	–	–	–	−0.19	–	–	–	−0.3	–
θ_{e_ALT}	–	–	–	0.12	–	–	–	0.66	–	–	–	0.6
θ_{in_ALT}	–	–	–	0.07	–	–	–	0.31	–	–	–	0.48
θ_{out_ALT}	–	–	–	−0.56	–	–	–	−0.74	–	–	–	−0.55

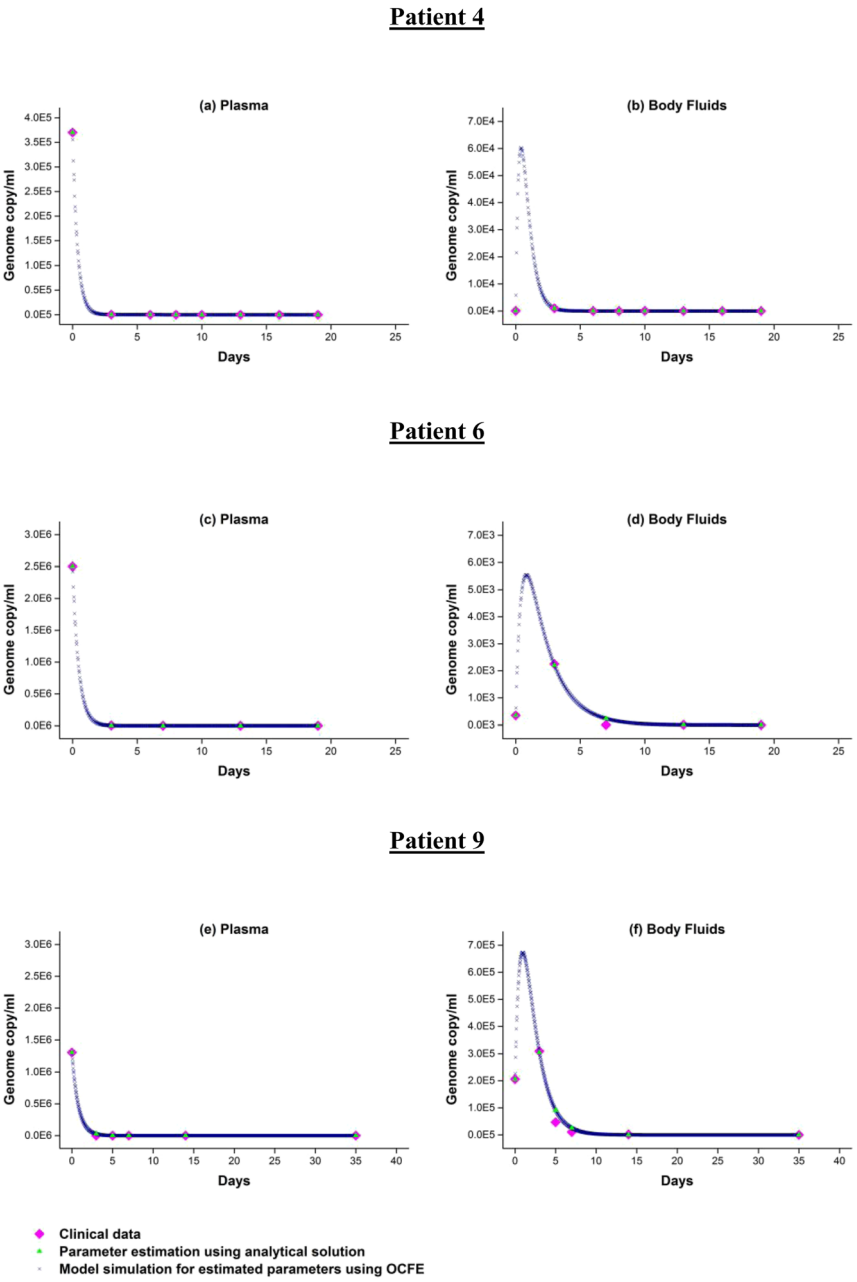

Figure 14.4: Pharmacokinetic analysis, individually for each patient – comparison of the PK model predictions (using an absolute objective function) with the clinical data.

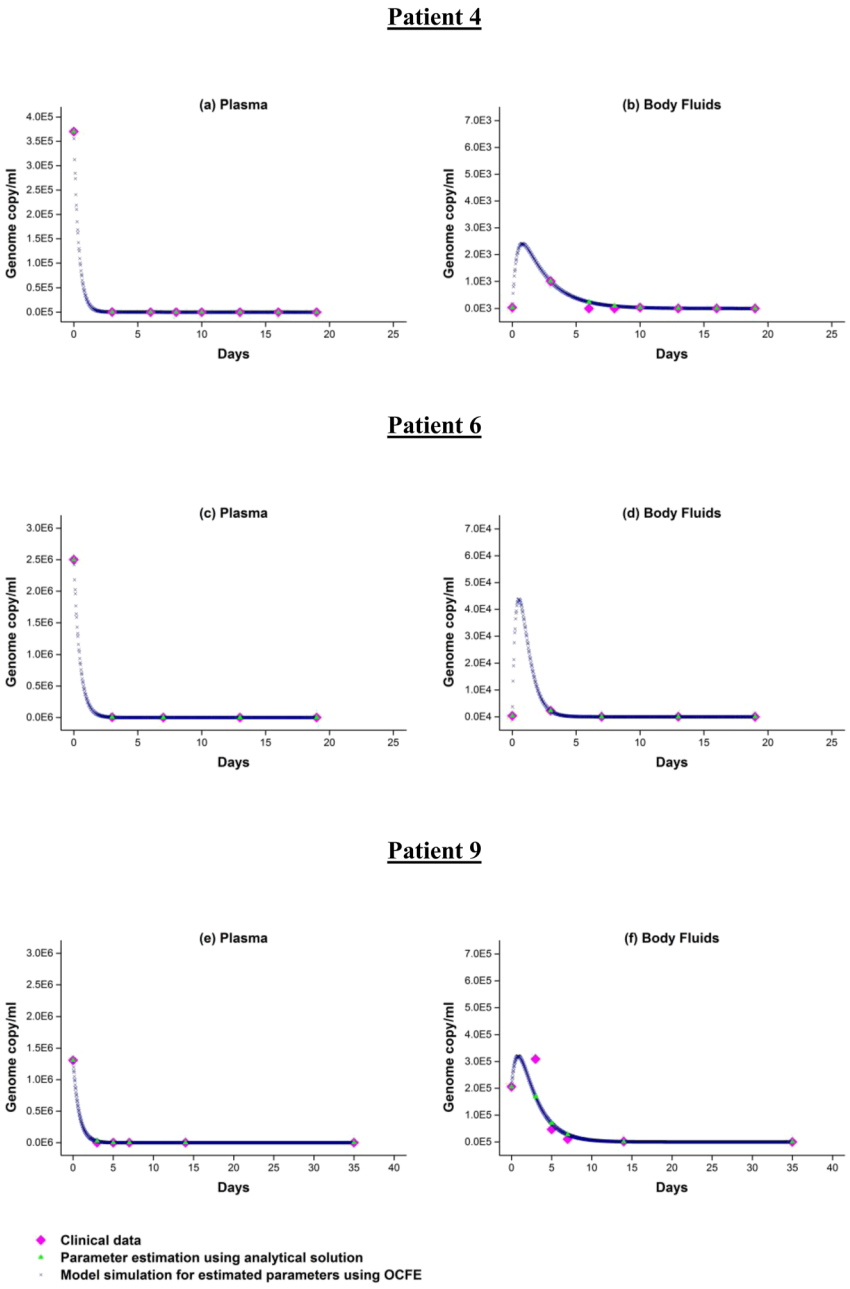

Figure 14.5: Pharmacokinetic analysis, individually for each patient – comparison of the PK model predictions (using a scaled objective function) with the clinical data.

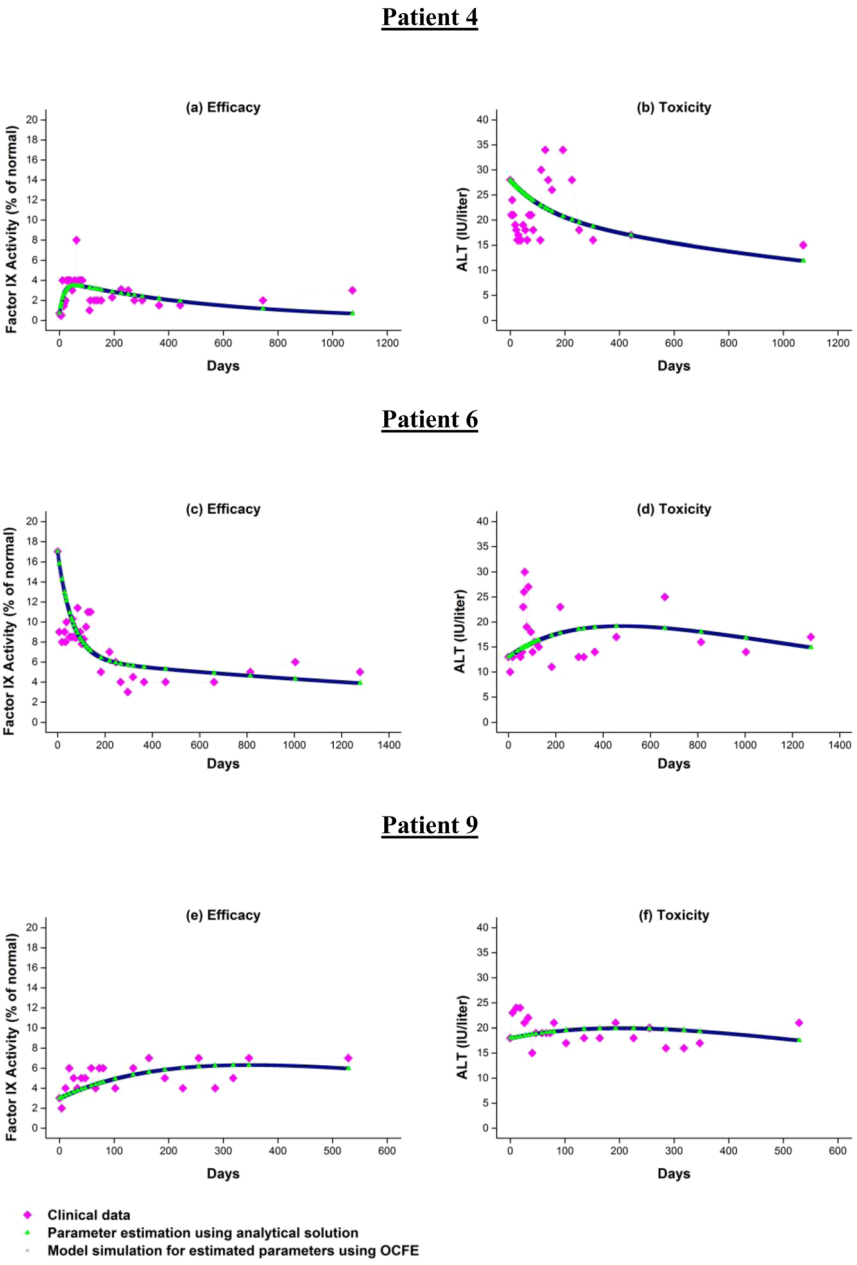

Figure 14.6: Pharmacodynamic analysis, individually for each patient – comparison of the PD model predictions (using an absolute objective function) with the clinical data.

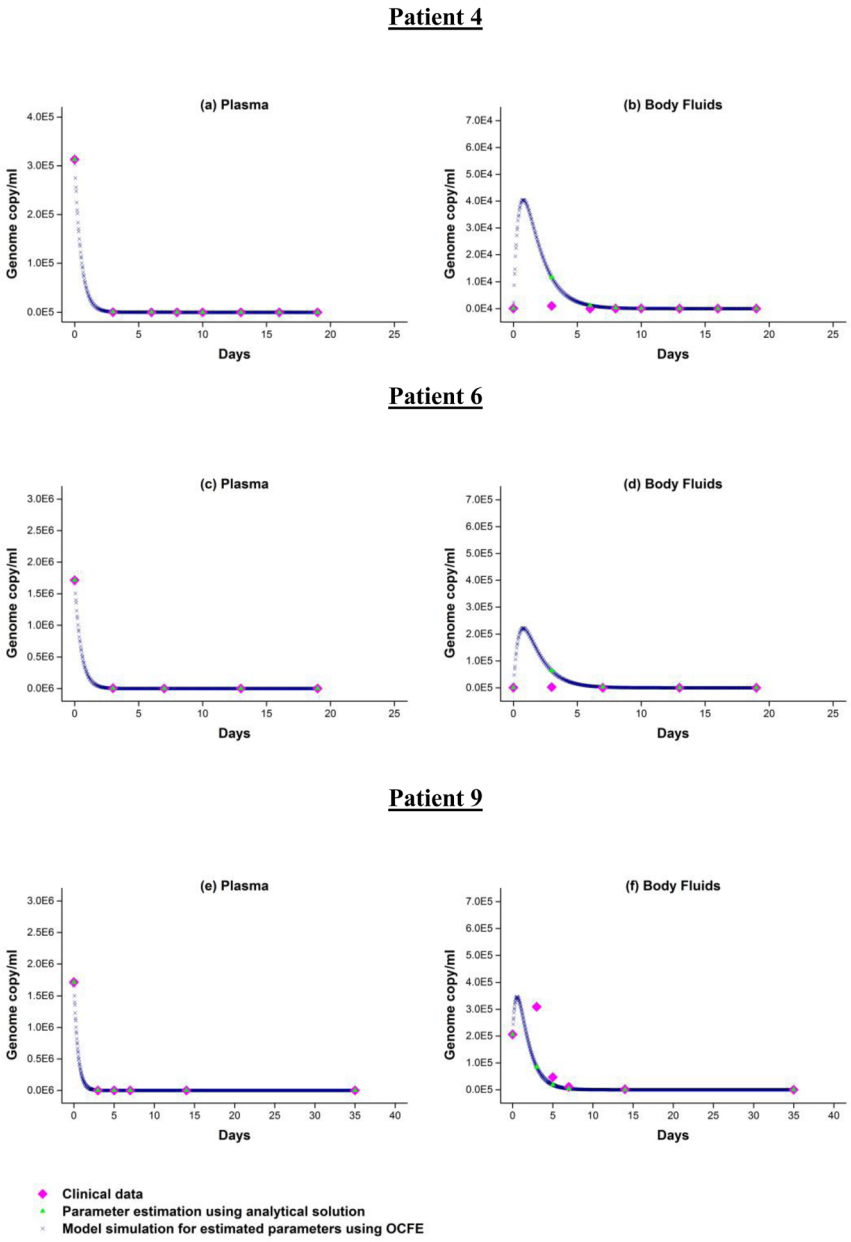

Figure 14.7: Pharmacokinetic analysis, for all patients simultaneously – comparison of the PK model predictions (using an absolute objective function) with the clinical data.

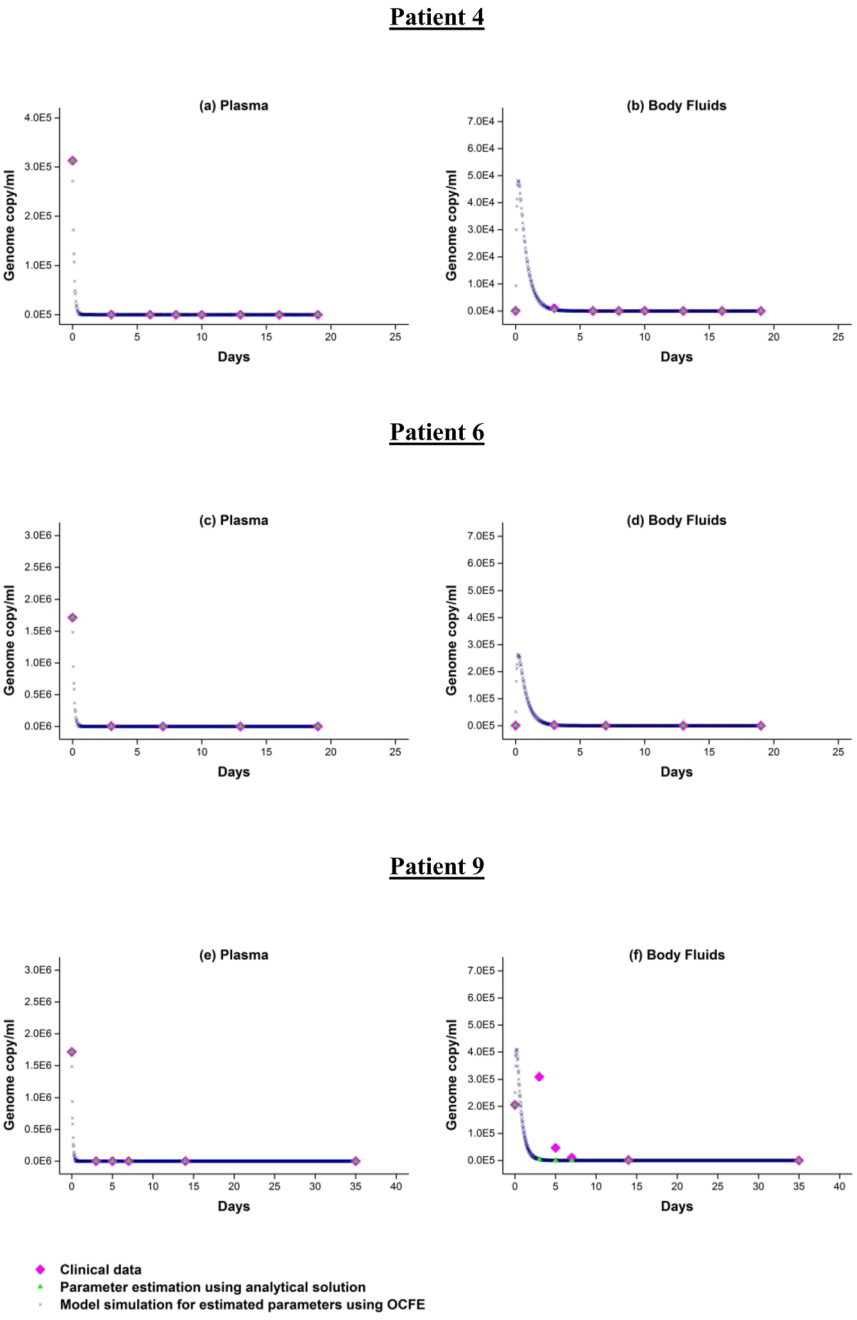

Figure 14.8: Pharmacokinetic analysis, for all patients simultaneously – comparison of the PK model predictions (using a scaled objective function) with the clinical data.

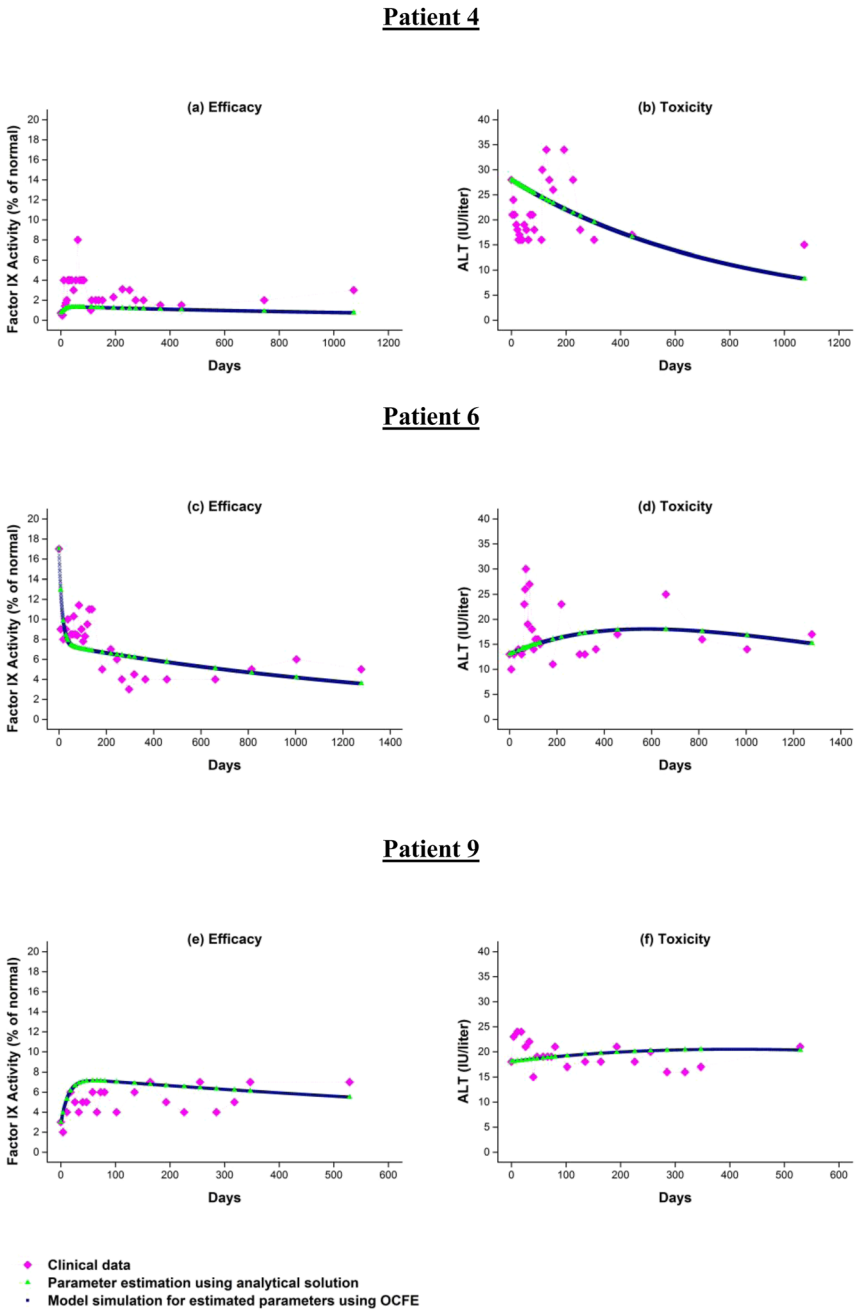

Figure 14.9: Pharmacodynamic analysis, for all patients simultaneously – comparison of the PD model predictions (using an absolute objective function) with the clinical data.

Table 14.7: Computational results for the individual modelling approach.

Patient 4		
	Objective function values	**Corresponding figures**
PK model	$Err_{absolute} = 1.2013 \times 10^{-5}$	Figure 14.4(a) and (b)
	$Err_{scaled} = 1.667 \times 10^{-16}$	Figure 14.5(a) and (b)
PD model – FIX	$Err_{absolute} = 52.140$	Figure 14.6(a)
PD model – ALT	$Err_{absolute} = 1{,}399.890$	Figure 14.6(b)
Patient 6		
	Objective function values	**Corresponding figures**
PK model	$Err_{absolute} = 1.0396 \times 10^{-5}$	Figure 14.4(c) and (d)
	$Err_{scaled} = 2.990$	Figure 14.5(c) and (d)
PD model – FIX	$Err_{absolute} = 200.021$	Figure 14.6(c)
PD model – ALT	$Err_{absolute} = 799.967$	Figure 14.6(d)
Patient 9		
	Objective function values	**Corresponding figures**
PK model	$Err_{absolute} = 3 \times 10^{-1}$	Figure 14.4(e) and (f)
	$Err_{scaled} = 2.997$	Figure 14.5(e) and (f)
PD model – FIX	$Err_{absolute} = 37.134$	Figure 14.6(e)
PD model – ALT	$Err_{absolute} = 187.068$	Figure 14.6(f)

Table 14.8: Computational results for the population modelling approach.

Patients 4, 6, and 9		
	Objective function values	**Corresponding figures**
PK model	$Err_{absolute} = 1{,}481.198$	Figure 14.7
	$Err_{scaled} = 10.270$	Figure 14.8
PD model – FIX	$Err_{absolute} = 1{,}011.102$	Figure 14.9(a), (c), and (e)
PD model – ALT	$Err_{absolute} = 4{,}167.984$	Figure 14.9(b), (d), and (f)

fluctuations in the PD clinical data. Another potential contributor is the existence of hypothetical effect compartment that acts as a link between the PK and PD models. However, the analysis shows that a good match is obtained between the clinical data and the model predictions. The pharmacokinetic analysis in this work demonstrates how the overall performance of the PK parameter estimation problem depends on the optimisation algorithms and the objective functions. Making such comparisons between an absolute objective function and a scaled objective function leads to the fact that using a scaling factor may cause an algorithm to determine a different optimal solution. The absolute and scaled objective function values vary with no observable trend. Hence,

based on a trade-off between the objective function values and the simulation results, a decision is made to use a set of parameters for subsequent computational studies.

14.3.2 Initial dose selection

This section aims to explore how the simulation-based modelling approach can assist in the initial dose selection. In this work, the initial doses used for the simulations are calculated based on the following assumptions: (i) the average plasma volume is 50 mL/kg [32] and (ii) there is a linear relationship between the dose administered (after conversion from vg/kg to vg/mL) and the initial vector concentration in plasma.

Linear regression is one of the most commonly used techniques to investigate the relationship between two quantitative variables [33]. Therefore, a linear regression analysis was carried out to determine the equation of the regression line, which is as follows and shown in Figure 14.10: Initial vector concentration in plasma = $5 \times 10^{-5} \times$ Dose − 287,000.

For comparison purposes, the dynamic simulations were carried out for different time periods and for various initial bolus doses. The PK/PD profiles are shown in Figures 14.11–14.14.

As can be seen in Figures 14.11b, 14.12b, 14.13b, and 14.14b, the vector is expected to be eliminated from the body within 10 days after administration. The simulation results (Figures 14.11–14.14) demonstrated that the increase in both factor IX activity and ALT level is dose-dependent, which is one of the key findings that is consistent with the work by Nathwani et al. [7]. In a recent study by Nathwani and Tuddenham [34], the authors reported that the highest level of transgene expression of between 8 % and 12 % of normal

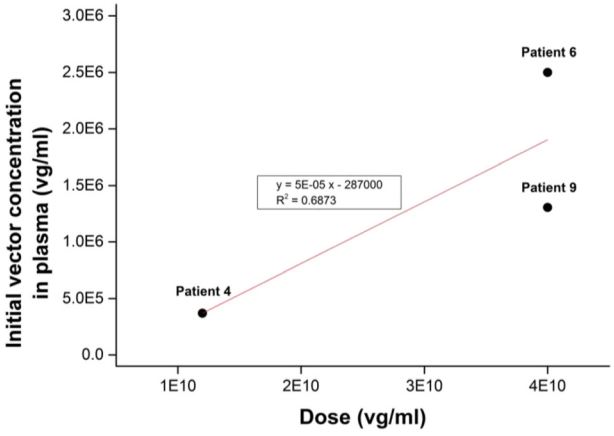

Figure 14.10: Linear regression curve between the dose administered and the initial vector concentration in plasma.

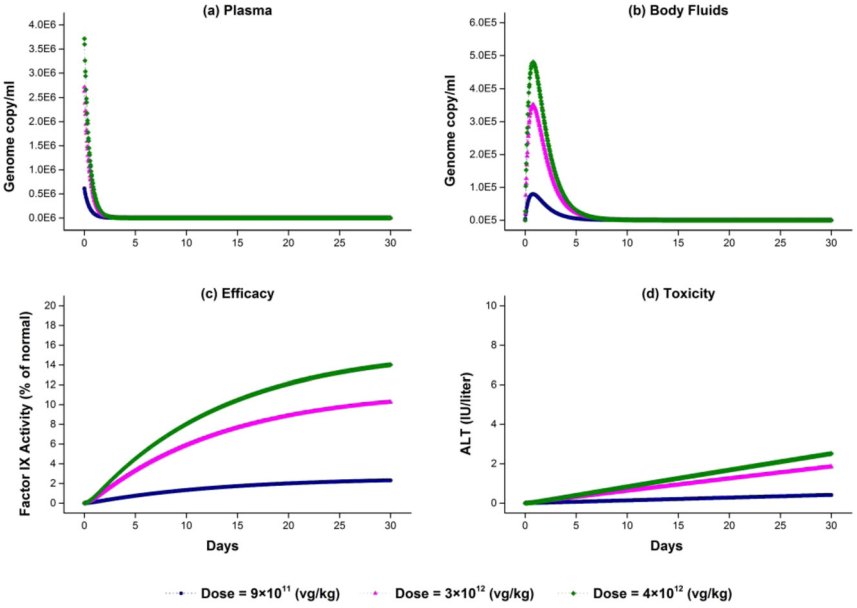

Figure 14.11: Population pharmacokinetic and pharmacodynamic results over a period of 30 days for different initial bolus doses.

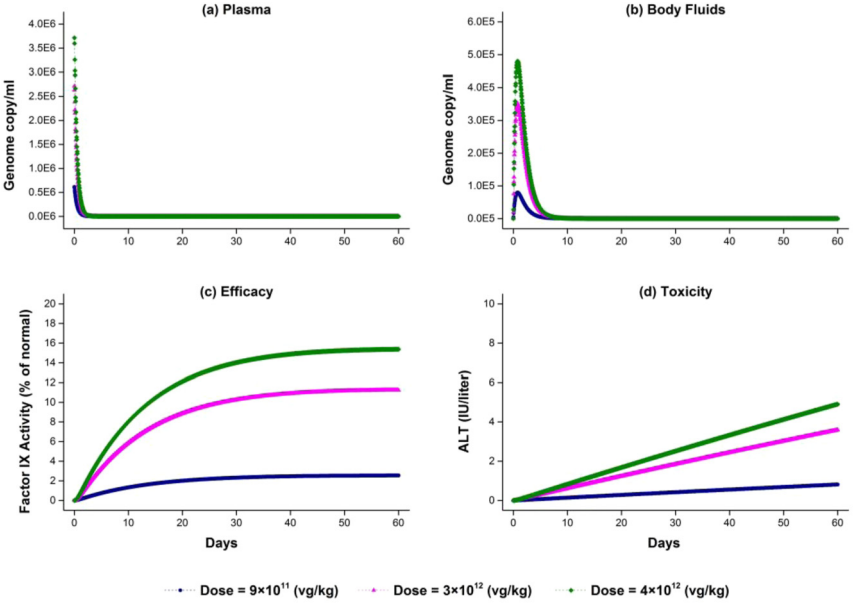

Figure 14.12: Population pharmacokinetic and pharmacodynamic results over a period of 60 days for different initial bolus doses.

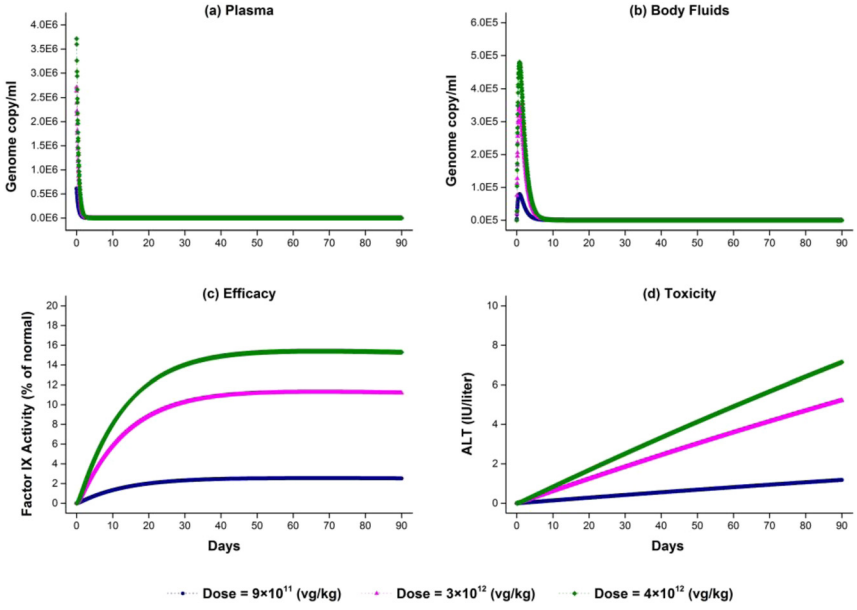

Figure 14.13: Population pharmacokinetic and pharmacodynamic results over a period of 90 days for different initial bolus doses.

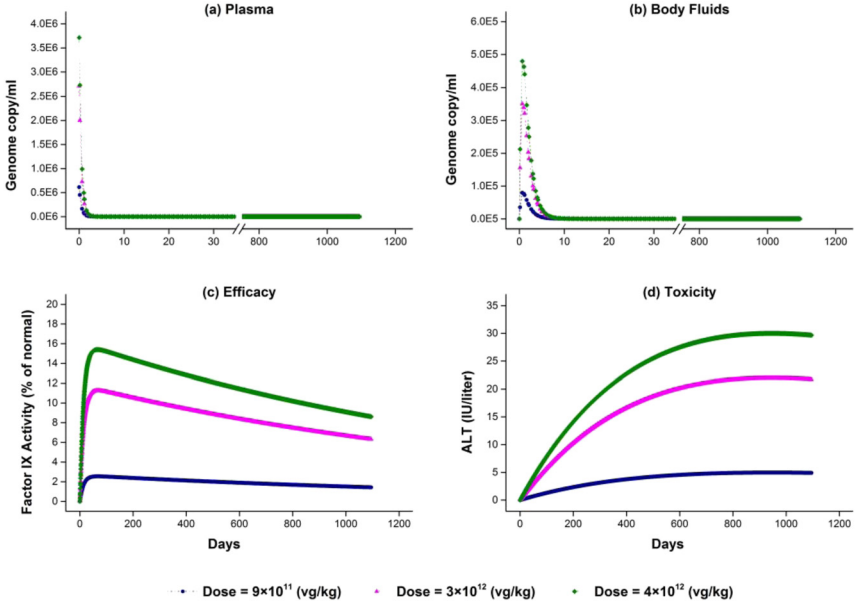

Figure 14.14: Population pharmacokinetic and pharmacodynamic results over a period of 3 years for different initial bolus doses.

was observed in the patients treated at the dose level of 2×10^{12} vg/kg, which remained stable up to 6 weeks after gene transfer. The simulation results in this chapter (Figures 14.12c, 14.13c, and 14.14c) lead to similar conclusion where FIX activity levels between 11 % and 15 % of normal can be observed for the high-dose subjects (dose level of 3×10^{12} vg/kg and 4×10^{12} vg/kg), which remained stable within 3 months after infusion. However, the ALT levels are increased consistently, especially in higher dose cohorts, which subsequently leads to a relative reduction in factor IX levels (about 55 % reduction). According to Nathwani et al. [7], the increase in the ALT level is associated with a decline in factor IX activity levels, suggesting a loss of transduced hepatocytes. Despite the drop in the level of expression, the simulation analysis found evidence for long-term efficacy as the FIX expression levels are maintained in the 6–10 % range in the high-dose patients within a period of 3 years (Figure 14.14c), suggesting a reduction in FIX concentrate usage. This is in line with the findings reported by Nathwani and Tuddenham [34], demonstrating that the transgenic FIX activity levels have remained stable over a period of 10 years follow-up and reduced the need for treatments with FIX concentrates.

14.4 Conclusions

In this chapter, a mathematical modelling approach was developed for gene transfer of adeno-associated viral vectors in patients with haemophilia B. The model-based platform discussed in this chapter incorporates the pharmacokinetics and pharmacodynamics of the scAAV2/8-LP1-hFIXco vectors. The PK/PD model parameters were estimated using the analytical solution of the model, individually for each patient in a dose-independent manner and for all patients simultaneously in a dose-dependent manner. A number of dynamic simulations were also carried out using OCFE for the validation of the model, demonstrating the simulation results are comparable to that obtained from parameter estimation. The simulation-based PK/PD modelling approach was then used for the initial dose selection to provide clinicians with better tools to make the decision-making process simpler for designing more effective treatment plans, which can be tailored to maximise efficacy while minimising toxicity for individual patients.

Acknowledgements: The authors would like to thank the editors David Bogle and Tomasz Sosnowski for their guidance and review of this article before its publication.

References

1. Jamili E, Nathwani AC, Dua V. Mathematical modelling of gene delivery in patients with haemophilia B. Chem Eng Sci 2023;281:119073.
2. George LA, Sullivan SK, Giermasz A, Rasko JEJ, Samelson-Jones BJ, Ducore J, et al. Hemophilia B gene therapy with a high-specific-activity factor IX variant. N Engl J Med 2017;377:2215–27.

3. Ramaswamy S, Tonnu N, Tachikawa K, Limphong P, Vega JB, Karmali PP, et al. Systemic delivery of factor IX messenger RNA for protein replacement therapy. Proc Natl Acad Sci USA 2017;114:E1941–E19.
4. Patel N, Reiss U, Davidoff AM, Nathwani AC. Progress towards gene therapy for haemophilia B. Int J Hematol 2014;99:372–6.
5. Powell JS, Pasi KJ, Ragni MV, Ozelo MC, Valentino LA, Mahlangu JN, et al. Phase 3 study of recombinant factor IX Fc fusion protein in hemophilia B. N Engl J Med 2013;369:2313–23.
6. Manno CS, Arruda VR, Pierce GF, Glader B, Ragni M, Rasko J, et al. Successful transduction of liver in hemophilia by AAV-Factor IX and limitations imposed by the host immune response. Nat Med 2006;12: 342–7.
7. Nathwani AC, Reiss UM, Tuddenham EGD, Rosales C, Chowdary P, McIntosh J, et al. Long-term safety and efficacy of factor IX gene therapy in hemophilia B. N Engl J Med 2014;371:1994–2004.
8. Nathwani AC, Davidoff A, Hanawa H, Zhou JF, Vanin EF, Nienhuis AW. Factors influencing in vivo transduction by recombinant adeno-associated viral vectors expressing the human factor IX cDNA. Blood 2001;97:1258–65.
9. Nathwani AC, Davidoff AM, Tuddenham EGD. Gene therapy for hemophilia. Hematol Oncol Clin N Am 2017; 31:853–68.
10. Nathwani AC, Gray JT, McIntosh J, Ng CYC, Zhou JF, Spence Y, et al. Safe and efficient transduction of the liver after peripheral vein infusion of self- complementary AAV vector results in stable therapeutic expression of human FIX in nonhuman primates. Blood 2007;109:1414–21.
11. Nathwani AC, Gray JT, Ng CYC, Zhou JF, Spence Y, Waddington SN, et al. Self-complementary adeno-associated virus vectors containing a novel liver-specific human factor IX expression cassette enable highly efficient transduction of murine and nonhuman primate liver. Blood 2006;107:2653–61.
12. Nathwani AC, Rosales C, McIntosh J, Rastegarlari G, Nathwani D, Raj D, et al. Long-term safety and efficacy following systemic administration of a self- complementary AAV vector encoding human FIX pseudotyped with serotype 5 and 8 capsid proteins. Mol Ther 2011;19:876–85.
13. Nathwani AC, Tuddenham EGD, Rangarajan S, Rosales C, McIntosh J, Linch DC, et al. Adenovirus-associated virus vector-mediated gene transfer in hemophilia B. N Engl J Med 2011;365:2357–65.
14. Ledley TS, Ledley FD. Multicompartment, numerical-model of cellular events in the pharmacokinetics of gene therapies. Hum Gene Ther 1994;5:679–91.
15. Banks GA, Roselli RJ, Chen R, Giorgio TD. A model for the analysis of nonviral gene therapy. Gene Ther 2003; 10:1766–75.
16. Varga CM, Hong K, Lauffenburger DA. Quantitative analysis of synthetic gene delivery vector design properties. Mol Ther 2001;4:438–46.
17. Varga CM, Tedford NC, Thomas M, Klibanov AM, Griffith LG, Lauffenburger DA. Quantitative comparison of polyethylenimine formulations and adenoviral vectors in terms of intracellular gene delivery processes. Gene Ther 2005;12:1023–32.
18. Dinh AT, Pangarkar C, Theofanous T, Mitragotri S. Understanding intracellular transport processes pertinent to synthetic gene delivery via stochastic simulations and sensitivity analyses. Biophys J 2007;92: 831–46.
19. Horobin RW, Weissig V. A QSAR-modeling perspective on cationic transfection lipids. 1. predicting efficiency and understanding mechanisms. J Gene Med 2005;7:1023–34.
20. Jandt U, Shao S, Wirth M, Zeng AP. Spatiotemporal modeling and analysis of transient gene delivery. Biotechnol Bioeng 2011;108:2205–17.
21. Berraondo P, Gonzalez-Aseguinolaza G, Troconiz IF. Semi-mechanistic pharmacodynamic modelling of gene expression and silencing processes. Eur J Pharmaceut Sci 2009;37:418–26.
22. Martin TM, Wysocki BJ, Wysocki TA, Pannier AK. Identifying intracellular pDNA losses from a model of nonviral gene delivery. IEEE Trans NanoBiosci 2015;14:455–64.
23. Jamili E, Dua V. Optimal model-based control of non-viral siRNA delivery. Biotechnol Bioeng 2018;115: 1866–77.

24. Holz M, Fahr A. Compartment modeling. Adv Drug Deliv Rev 2001;48:249–64.
25. Nestorov I. Whole body pharmacokinetic models. Clin Pharmacokinet 2003;42:883–908.
26. Howard EL, Becker KCD, Rusconi CP, Becker RC. Factor IXa inhibitors as novel anticoagulants. Arterioscler Thromb Vasc Biol 2007;27:722–7.
27. Tsang TC, Bentley DR, Mibashan RS, Giannelli F. A factor-IX mutation, verified by direct genomic sequencing, causes haemophilia-B by a novel mechanism. EMBO J 1988;7:3009–15.
28. Franchini M, Frattini F, Crestani S, Bonfanti C. Haemophilia B: current pharmacotherapy and future directions. Expet Opin Pharmacother 2012;13:2053–63.
29. Gabrielsson J, Weiner D. Pharmacokinetic and pharmacodynamic data analysis: concepts and applications, 4th ed. Sweden: Swedish Pharmaceutical Press; 2010.
30. Washington IM, Van Hoosier G. Clinical biochemistry and hematology. In: Suckow MA, Stevens KA, Wilson RP, editors. The laboratory rabbit, guinea pig, hamster, and other rodents. American college of laboratory animal medicine series. San Diego: Elsevier Academic Press Inc; 2012:57–116 pp.
31. Degasperi A, Fey D, Kholodenko BN. Performance of objective functions and optimisation procedures for parameter estimation in system biology models. NPJ Syst Biol Appl 2017;3:20.
32. Yiengst MJ, Shock NW. Blood and plasma volume in adult males. J Appl Physiol 1962;17:195.
33. Bewick V, Cheek L, Ball J. Statistics review 7: correlation and regression. Crit Care 2003;7:451–9.
34. Nathwani AC, Tuddenham EGD. Haemophilia, the journey in search of a cure. 1960-2020. Br J Haematol 2020;191:573–8.

Supplementary Material: This article contains supplementary material (https://doi.org/10.1515/psr-2024-0057).